

Magnetolectric gyration effect in $Tb_{1-x}Dy_xFe_{2-y}Pb(Zr,Ti)O_3$ laminated composites at the electromechanical resonance

Shuxiang Dong, Junyi Zhai, J. F. Li, D. Viehland, and M. I. Bichurin

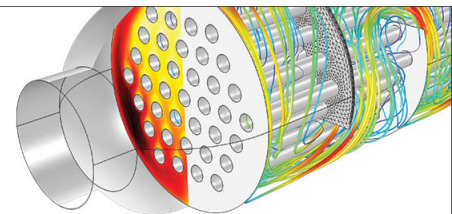
Citation: [Applied Physics Letters](#) **89**, 243512 (2006); doi: 10.1063/1.2404977

View online: <http://dx.doi.org/10.1063/1.2404977>

View Table of Contents: <http://scitation.aip.org/content/aip/journal/apl/89/24?ver=pdfcov>

Published by the [AIP Publishing](#)

Over **700** papers &
presentations on
multiphysics simulation



VIEW NOW ►

 COMSOL

Magnetoelectric gyration effect in Tb_{1-x}Dy_xFe_{2-y}/Pb(Zr,Ti)O₃ laminated composites at the electromechanical resonance

Shuxiang Dong,^{a)} Junyi Zhai, J. F. Li, and D. Viehland

Department of Materials Science and Engineering, Virginia Tech, Blacksburg, Virginia 24061

M. I. Bichurin

Institute of Electronic and Informative Systems, Novgorod State University, 173003 Veliky Novgorod, Russia

(Received 9 August 2006; accepted 2 November 2006; published online 14 December 2006)

A giant current-to-voltage (*I-V*) gyration effect was found in magnetostrictive Tb_{1-x}Dy_xFe_{2-y} and piezoelectric Pb(Zr,Ti)O₃ laminated composites. An equivalent circuit theory was developed for magnetoelectric gyration, which predicted that *I-V* conversion is reduced by a frequency transfer function $Z_R(f)$ and that the maximum occurs at resonance. A giant conversion coefficient up to 2500 V/A was predicted and confirmed. © 2006 American Institute of Physics. [DOI: 10.1063/1.2404977]

The magnetolectric (ME) effect is a polarization response to an applied magnetic field *H* or vice versa. It has potential applications as highly sensitive magnetic and/or electric current sensors,^{1,2} transformers,³ and electric-field tunable microwave resonators.⁴ ME materials have been found in single phases,⁵ and in multiphase systems consisting of piezoelectric and magnetostrictive components.⁶⁻¹⁸ By far the highest ME effects have been reported for magnetostrictive/piezoelectric two-phase laminated composites,^{1-3,11,14-16,19} connected in either longitudinally magnetized and transversely poled (*L-T*) (Refs. 1, 11, and 14) or (*L-L*) (Refs. 15, 16, 19, and 20) configurations.

Analysis of ME effects in magnetostrictive/piezoelectric two-phase composites has been performed using constitutive equations and a composite averaging method.^{17,18} Recently,^{16,20} an alternate equivalent circuit approach for analyzing ME effects in magnetostrictive/piezoelectric laminates was reported. Near the electromechanical resonance frequency, analysis predicted a large ME voltage gain^{3,20} (i.e., the induced output voltage from the piezolayer is much higher than an input voltage applied to the magnetic coils used to excite the Terfenol-D layers). In this prior analysis, we failed to obtain the *I-V* conversion relations: this could be important for device applications in power electronics,²¹ current sensors,²² and filters.²³ However, since that time, we have come across early reports concerning *gyrators* in electromechanical and magnetomechanical transductions.²⁴ An *ideal gyrator* was proposed in 1948 by Tellegen,²⁵ and is a network component that acts as antireciprocal couple.

In this letter, we consider a long-type ME laminate,^{4,20} consisting of a single piezoelectric PbZr_xTi_{1-x}O₃ (PZT) layer symmetrically poled along its length direction and that is sandwiched between two Tb_{1-x}Dy_xFe₂ (Terfenol-D) ones magnetized in their length direction. This laminate is illustrated in Fig. 1(a) and is designated as the “push-pull” configuration. We will show that this piezoelectric/magnetostrictive two-phase laminated composite has a giant *I-V* conversion due to gyration: where the gyration efficiency is reduced from its ideal value—except in the vicinity of the

electromechanical resonance—by a frequency transfer function $Z_R(f)$.

Our approach was founded on piezoelectric and magnetostrictive constitutive equations,^{16,20} mutually coupled to each other through elastic strain *S*(*z*) and stress *T*(*z*). An equation of motion, driven by an ac *I*_{in} input to the coils, was used to couple the two constitutive equations. Due to elastic

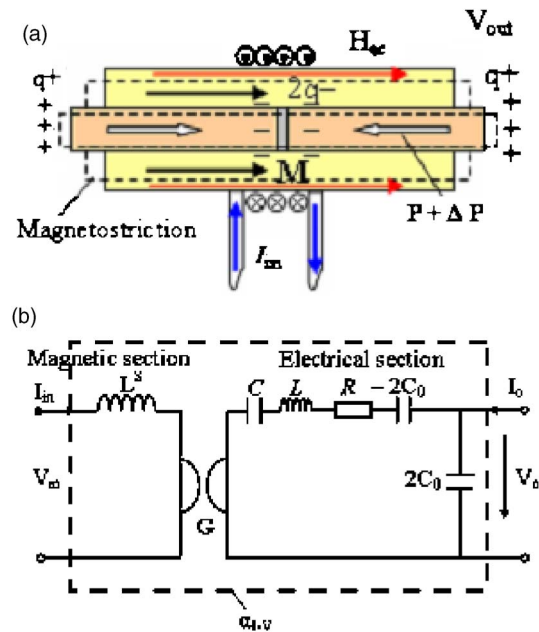


FIG. 1. (Color online) (a) Illustrations of ME *I-V* conversion in Terfenol-D/PZT laminate that is driven by a turn coil, with input current of I_{in} . The input I_{in} produces an ac magnetic field H_{ac} that in turn excites magnetostrictive strains in Terfenol-D layers, then forcing the laminated piezoelectric PZT layer to strain longitudinally, and resulting in a polarization change ΔP and net free charges $q+$ at the two end electrodes and $2q-$ at middle electrode of the piezoelectric layer. Finally, the applied I_{in} produces an output voltage V_{out} across the piezoelectric layer, realizing ME *I-V* conversion. (b) Equivalent circuit model of ME gyrator under resonance drive and free condition, where $G = \varphi_m / \varphi_p$; $\varphi_m = NA_m d_{33,m} / s_{33}^H I$; $\varphi_p = 2A_p g_{33,p} / l s_{33}^D \bar{\beta}_{33}$; $L^s = \mu^s N^2 A_m / l$; $R = \pi Z_0 / 8 Q_m \varphi_p^2$; $L = \pi Z_0 / 8 \omega_s \varphi_p^2$; $C = \varphi_p^2 / \omega_s^2 L_{mech}$; $C_0 = 2A_p / l \bar{\beta}_{33}$; $Z_0 = \bar{\rho} \bar{v} A_{lam}$; and $\omega_s = \pi \bar{v} / l$. The parameters A_m , A_p , and A_{lam} are the cross-sectional areas of the magnetostrictive layers, piezoelectric layer, and laminate, respectively; l is the length of the laminate; $\bar{\rho}$ and \bar{v} are the mean density and acoustic velocity of the laminate; and μ^s is the magnetic permeability of the magnetostrictive layer under constant stress.

^{a)}Electronic mail: sdong@vt.edu

coupling to the magnetostrictive layers, the piezoelectric layer is also put into forced oscillation by I_{in} , generating a voltage across the two end electrodes and middle ground plane. Accordingly, the following relationships can be derived:

$$F_1 = -Z_1 \dot{u}_1 + \left[Z_2 + \frac{\varphi_p^2}{j\omega(-2C_o)} \right] (\dot{u}_1 - \dot{u}_2) + G\varphi_p I_{in} + \varphi_p V_{out}, \quad (1a)$$

$$F_2 = -Z_1 \dot{u}_2 + \left[Z_2 + \frac{\varphi_p^2}{j\omega(-2C_o)} \right] (\dot{u}_1 - \dot{u}_2) + G\varphi_p I_{in} + \varphi_p V_{out}, \quad (1b)$$

$$V_{in} = j\omega L^S I_{in} + G\varphi_p (\dot{u}_1 - \dot{u}_2), \quad (1c)$$

$$I_{out} = j\omega(2C_o) V_{out} + \varphi_p (\dot{u}_2 - \dot{u}_1), \quad (1d)$$

where F_1 and F_2 are the force phasors, \dot{u}_1 and \dot{u}_2 the mechanical velocities, V_{in} and I_{in} the input voltage and current applied to the coils, V_{out} and I_{out} the induced voltage and current from the piezoelectric layer, Z_1 and Z_2 the mechanical impedances; L^S the clamped inductance of the coil, C_o the static capacitance of the piezoelectric layer, φ_p the electro-mechanical coupling factor; ω the angular frequency, and G a special coupling or transfer factor, designated as the gyration coefficient.

Next, following Tellegen,²⁵ we introduce a passive four-terminal-network gyrator, where the voltage and current to input ends of the gyrator are I_1 and V_1 , and correspondingly those to the output ends are I_2 and V_2 . By definition, the gyrator satisfies the following relation: $V_1 = -GI_2$ and $V_2 = GI_1$, where G is the ideal gyrator coefficient of the ME laminate determined by the material parameters and composite configuration. An equivalent circuit model containing an ideal gyrator G , with negligible electric/magnetic dissipations and under free-boundary conditions, can then be obtained as given in Fig. 1(b). Over a narrow frequency range, we will consider G as independent of frequency f , but we must note that G will change some with frequency, as the permeability of Terfenol-D and the dielectric constant of PZT both decrease slightly with increasing f . Following this model, an applied I_1 (I_{in}) to the coils *gyrates* into an output voltage of V_2 (V_{out}) in the piezoelectric section, via G that acts as an impedance inverter. Alternatively, it is possible that a current I_2 input to the piezoelectric section could also *gyrate* into a voltage V_1 across the coils. Note that the network components (L , C , R , $2C_o$, and $-2C_o$) in this equivalent model act as a frequency transfer function, effectively reducing G and consequently limiting the apparent I - V conversion factor.

From Fig. 1(b), it is then straightforward to determine the I - V conversion coefficient that we designate as α_{I-V} . This is the ‘‘apparent gyration coefficient’’ of the ‘‘black box’’ outlined by dashed lines in the figure. Assuming the output to be in an open-circuit condition, this effective parameter α_{I-V} can be determined as

$$\alpha_{I-V} = \frac{V_{out}}{I_{in}} = Z_R(f)G; \quad G = \frac{NA_m d_{33,m} g_{33,p}}{2k_{33,p}^2 A_p s_{33}^H}, \quad (2a)$$

where $Z_R(f) = [1/j\omega(2C_o)]/R + j\omega L + 1/j\omega C$ is a ratio of output to input impedances in the electrical section of the

equivalent model of Fig. 1(b). Clearly, α_{I-V} is a nonideal gyration coefficient, reduced from its ideal value G by a frequency transfer function/factor $Z_R(f)$. At resonance, $\omega_s = \pi\bar{v}/l$ and $(1/j\omega C) + j\omega L = 0$; thus, the maximum I - V conversion coefficient is

$$\alpha_{I-V,max} = \frac{4\varphi_m \varphi_p Q_{m,eff}}{\pi C_o \omega_s Z_o} \quad (2b)$$

or,

$$V_{0,max} = \alpha_{I-V,max} I_{in} \quad (\text{at resonance}), \quad (2c)$$

where φ_m is the magnetoelastic coupling factors. The value of $V_{0,max}$ is linearly proportional to the input current I_{in} , and a high effective mechanical quality factor ($Q_{m,eff}$) results in large I - V conversion.

Calculations of (2) for G , $Z_R(f)$, and $\alpha_{I-V}(f)$ were then performed using previously reported material parameters.¹⁶ These calculations were done by assuming a Terfenol-D/PZT laminate length, width, and thickness of 70, 10, and 7 mm, respectively, a coil turn number of $N=100$, and an effective mechanical quality factor of $Q_{m,eff}=50$. Figure 2 shows the predicted values for G and $Z_R(f)$ in part A and $\alpha_{I-V}(f)$ in part B. It can be seen that (i) the ideal gyration coefficient $G=4830$ V/A is a constant (at a given frequency range), which is related only to the configuration of the ME laminate and to the material parameters of its layers; (ii) the frequency transfer function $Z_R(f)$ reduces the value of the gyration coefficient from its ideal value of G to an effective value of α_{I-V} ; and (iii) below the resonance frequency range the value of $Z_R(f)$ is small (0.02) resulting in a low value of α_{I-V} , whereas at resonance $Z_R(f)=0.64$ resulting a maximum value of $\alpha_{I-V}=3100$ V/A that is not too much lower than the ideal value of $G=4830$ V/A.

The ME voltage induced by I_{in} was then measured as a function of frequency over the bandwidth of 1–40 kHz. The voltage from the piezoelectric layer was directly read by an oscilloscope. Measurements were performed under a dc magnetic bias of $H_{dc}=200$ Oe, where the effective piezomagnetic coefficient of Terfenol-D is known to be maximum.¹⁹ As shown in Fig. 2(c), the I - V conversion factor was found to have a maximum value of $\alpha_{I-V}=2500$ V/A near a resonance frequency of $f_s=19.8$ kHz, consistent with predictions. Analysis of the data with (2) yielded a value of $Q_{m,eff} \approx 50$, in agreement with our assumption. We ignored the possibility of electric and magnetic losses in the circuit model analysis, but realized that their inclusion could yield even better correspondence between the calculated and measured values of α_{I-V} . From this I - V conversion data, a large ME voltage gain of ~ 330 (at resonance) was estimated. The induced ME voltage as a function of I_{in} applied to the coils was also measured, as shown in the inset of Fig. 2(c). It can be seen that the induced ME voltage was linear with respect to I_{in} over a wide range of input currents, as predicted by (2b). We also observed (i) reverse gyration: a I_2 of 57 μ A applied to the piezoelectric section induced a $V_1=73$ mV across a 100-turn coil. Apparently, the inverse gyration is smaller than direct I - V (I_1 -to- V_2) gyration, indicating that our current ME laminate is a nonideal construction; (ii) impedance inversion: a small resistor of $R_i=100$ Ω in parallel to the primary terminals of the gyrator G resulted in a decreased in the value of α_{I-V} to 2100 V/A, which occurs because R_i introduces an impedance G^2/R_i in series with the secondary terminals.

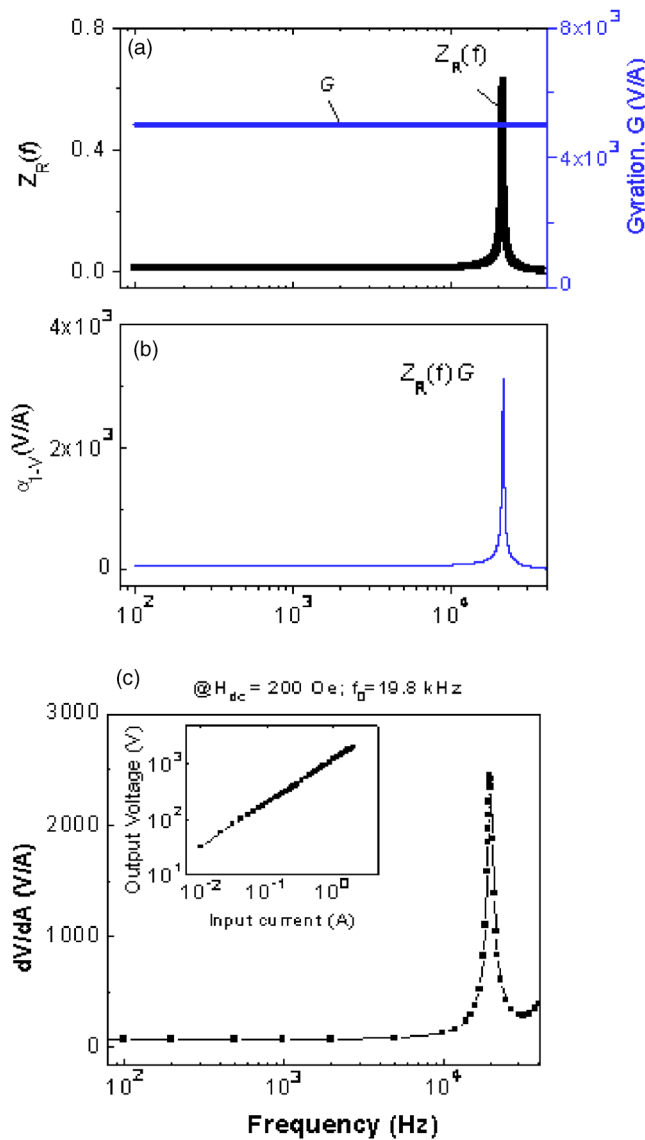


FIG. 2. (Color online) Calculations using Eq. (2) as a function of drive frequency f , for (a) the ideal gyration coefficient G and frequency transfer function $Z_R(f)$, and (b) I - V conversion coefficient α_{I-V} , as a function of f ; (c) experimental I - V conversion (or nonideal gyration coefficient) α_{I-V} as a function of f , where the inset shows the output voltage V_{out} gyrated from an input current I_{in} .

Clearly, our calculations and experiments demonstrate that the two-phase PZT/Terfenol-D laminated composite is a ME gyration with giant I - V gyration ability at resonance.

In summary, a giant I - V gyration effect based on ME coupling was found in two-phase PZT/Terfenol-D laminate

composites. The observed ME gyration coefficient α_{I-V} was reduced from the ideal value G by a frequency transfer function, and exhibited a maximum at the electromechanical resonance frequency. A giant conversion coefficient of up to 2500 V/A was predicted and confirmed. We hope that these findings will stimulate the development of miniature power conversion and other devices based on ME coupling.

This work was supported in full by the Office of Naval Research.

- ¹S. X. Dong, J. F. Li, and D. Viehland, Appl. Phys. Lett. **83**, 2265 (2003); **85**, 2307 (2004).
- ²S. X. Dong, J. G. Bai, J. Y. Zhai, J.-F. Li, G.-Q. Lu, D. Viehland, S. Zhang, and T. R. Shrout, Appl. Phys. Lett. **86**, 182506 (2005).
- ³S. X. Dong, J. F. Li, and D. Viehland, Appl. Phys. Lett. **84**, 4188 (2004); **85**, 3534 (2004).
- ⁴M. Bichurin, V. Petrov, Yu. Kiliba, and G. Srinivasan, Phys. Rev. B **66**, 134404 (2002); M. Bichurin, I. Kornev, V. Petrov, A. Tatarsenko, Y. Kiliba, and G. Srinivasan, *ibid.* **64**, 094409 (2001).
- ⁵S. Di Matteo and A. G. M. Jansen, Phys. Rev. B **66**, 100402 (2002); I. E. Dzyaloshinskii, Sov. Phys. JETP **37**, 628 (1960).
- ⁶L. Wiegelmann, A. A. Stepanov, I. M. Vitebsky, A. G. M. Jansen, and P. Wyder, Phys. Rev. B **49**, 10039 (1994).
- ⁷J. Van Suchtelen, Philips Res. Rep. **27**, 28 (1972).
- ⁸C. W. Nan, L. Liu, N. Cai, J. Zhai, Y. Ye, and Y. H. Lin, Appl. Phys. Lett. **81**, 3831 (2002).
- ⁹G. Srinivasan, E. Rasmussen, B. Levin, and R. Hayes, Phys. Rev. B **65**, 134402 (2002); **64**, 214408 (2001).
- ¹⁰G. Srinivasan, V. M. Laletin, R. Hayes, N. Puddubnaya, E. T. Rasmussen, D. J. Fekel, Solid State Commun. **124**, 373 (2002).
- ¹¹J. G. Wan, Z. Y. Li, Y. Wang, M. Zeng, G. H. Wang, and J.-M. Liu, Appl. Phys. Lett. **86**, 202504 (2005); J. G. Wan, J.-M. Liu, H. L. W. Chand, C. L. Choy, G. H. Wang, and C. W. Nan, J. Appl. Phys. **93**, 9916 (2003).
- ¹²M. I. Bichurin, V. M. Petrov, and G. Srinivasan, Phys. Rev. B **68**, 054402 (2003).
- ¹³K. Mori and M. Wuttig, Appl. Phys. Lett. **81**, 100 (2002).
- ¹⁴S. X. Dong, J. F. Li, and D. Viehland, J. Appl. Phys. **95**, 2625 (2004); IEEE Trans. Ultrason. Ferroelectr. Freq. Control **50**, 1236 (2003).
- ¹⁵S. X. Dong, J. F. Li, and D. Viehland, Appl. Phys. Lett. **83**, 4812 (2003); **85**, 5305 (2004); J. Appl. Phys. **96**, 3382 (2004).
- ¹⁶S. X. Dong, J. F. Li, and D. Viehland, IEEE Trans. Ultrason. Ferroelectr. Freq. Control **50**, 1253 (2003); **51**, 794 (2004).
- ¹⁷C. W. Nan, Ming Li, and Jin H. Huang, Phys. Rev. B **63**, 144415 (2001).
- ¹⁸M. Avellaneda and G. Harshe, J. Low Temp. Phys. **5**, 501 (1994).
- ¹⁹S. X. Dong, J. Zhai, F. Bai, J. F. Li, and D. Viehland, Appl. Phys. Lett. **87**, 062502 (2005).
- ²⁰S. X. Dong, J. Mater. Sci. **41**, 97 (2006).
- ²¹A. Zeki, and A. Toker, Int. J. Electron. **59**, 59 (2005).
- ²²Sergio Franco, *Design with Operational Amplifiers and Analog Integrated Circuits*, 3rd ed. (McGraw-Hill, New Delhi, 2002), p. 60.
- ²³B. Guthrie, J. Hughes, T. Sayers, and A. Spencer, IEEE J. Solid-State Circuits **40**, 1872 (2005).
- ²⁴R. S. Wollett, *Sonar Transducer Fundamentals* (Naval Underwater Systems Command, Newport, RI, 1970), Sec. I, p. 156; J. Acoust. Soc. Am. **40**, 1112 (1966).
- ²⁵B. D. H. Tellegen, Philips Res. Rep. **3**, 81 (1948).